Interaction Notes

Note 397

April 1978

TRANSIENT CURRENT INJECTION INTO A RESISTIVE SHEET

K. F. Casey
The Dikewood Corporation
1613 University Boulevard, N.E.
Albuquerque, New Mexico 87102

Abstract

The transient injection of current into a resistive sheet of infinite transverse extent is considered. The surface current density in the sheet and the magnetic field just beneath the sheet are determined as functions of position and time. It is found that when the equivalent sheet resistance takes values characteristic of graphite-epoxy advanced composite or of the bonded-junction wire mesh screen often cured into one surface of a nonconductive composite, the surface current density in the sheet is practically indistinguishable from that which would exist if the sheet were perfectly conducting. The magnetic field beneath the sheet is small in comparison to that directly radiated by the injected current; its time dependence is shown to be proportional to the time derivative of the injected current waveform.

Research sponsored by the Air Force Office of Scientific Research, Air Force Systems Command, USAF, under Grant No. AFOSR-76-2980. The United States Government is authorized to reproduce and distribute reprints for governmental purposes.

CONTENTS

ILLUSTRATIONS

I. INTRODUCTION

In this note we consider the problem of determining the surface current density and the electromagnetic field produced by a transient current which is injected into a planar sheet of conductive material of infinite transverse extent. Our purpose is to gain some insight into the behavior of graphite-epoxy and screened nonconductive composite materials as shields against injected current-induced fields.

A graphite-epoxy panel can be modeled as an anisotropically conducting slab whose transverse conductivity is around 10^4 mho m^{-1} and whose normal conductivity is around 50 mho m^{-1} [1,2]. The panel is typically 1-3 mm thick. The bonded-mesh screen which can be used to improve the shielding effectiveness of a poorly conductive or nonconductive composite panel (e.g., a boron-epoxy composite) can be modeled as a equivalent sheet-impedance operator [3,4]. Over the frequency range where the reactive character of the screen can be ignored ($f \leq 10^6$ Hz), both the conductive composite and the bonded-mesh screen may be described as equivalent impedance sheets, with

$$Z_s = (\sigma d)_{eq}^{-1} \tag{1.1}$$

denoting the sheet impedance. $(\sigma d)_{eq}$ is the equivalent conductivity-thickness product of the conductive panel or the screen. Typical values for this quantity are in the range $10^1 - 10^2$ mhos.

In the following section (II) we formulate the problem in the frequency domain. The surface current density and the penetrating magnetic field are evaluated in sections III and IV. Section V concludes the note.

II. FORMULATION

The geometry of the problem is shown in Fig. 1. An impedance sheet of negligible thickness and infinite transverse extent is located in the plane z=0. An infinitely long filamentary current lies on the positive z-axis. In the time domain, the current is $i_o(t)$; the specific time dependence which we consider in this note is

$$i_o(t) = eI_p \frac{t}{\tau_o} e^{-t/\tau_o} U(t) \tag{2.1}$$

in which I_p denotes the peak current which occurs at $t=\tau_o$ and U(t) is the unit step function. We assume that $\tau_o \geq 10^{-6}$ sec, so that the reactive component of a mesh impedance can be neglected. A plot of $i_o(t)/I_p$ vs. t/τ_o is shown in Fig. 2. The objectives of the analysis are the determination of the surface current density in the sheet and the magnetic field in the region z<0.

In the frequency domain (the time dependence exp(st) is assumed), the electric and magnetic fields are given for ρ>0 by

$$\tilde{\bar{E}}(\bar{r},s) = \frac{1}{s\varepsilon_o} \nabla \times \nabla \times \tilde{\Psi} \bar{a}_z \tag{2.2a}$$

$$\tilde{\bar{H}}(\bar{r},s) = \nabla \times \tilde{\Psi} \bar{a}_z \tag{2.2b}$$

where $\tilde{\Psi}$ is a solution of

$$\frac{1}{\rho} \frac{\partial}{\partial \rho} \left(\rho \frac{\partial \tilde{\Psi}}{\partial \rho} \right) + \frac{\partial^2 \tilde{\Psi}}{\partial z^2} - \frac{s^2}{c^2} \tilde{\Psi} = 0 \tag{2.3}$$

and in which $c = (\mu_o \varepsilon_o)^{-1/2}$ denotes the speed of light in free space. $\tilde{\Psi}$ satisfies the following boundary conditions at z=0:

1. $\frac{\partial^2 \tilde{\Psi}}{\partial \rho \partial z}$ is continuous at z=0 (2.4a)

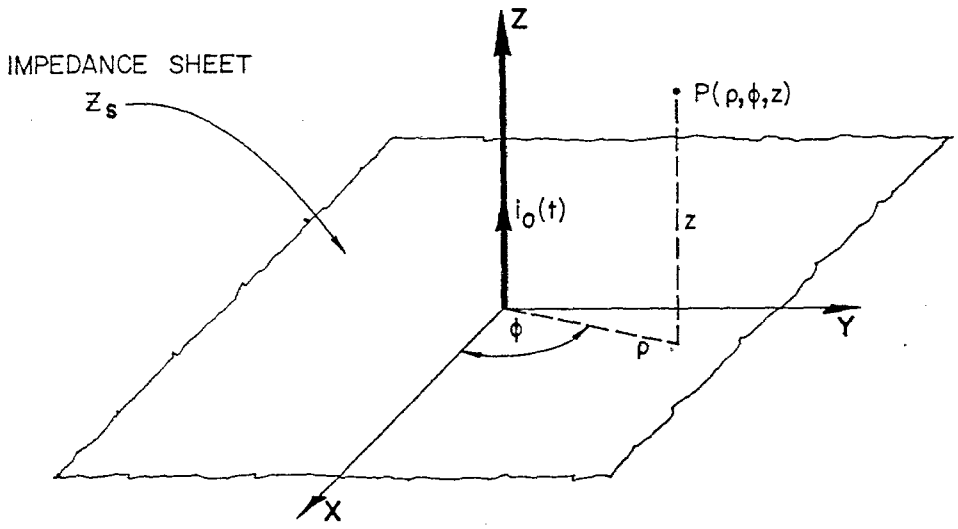

Figure 1. Geometry of the problem

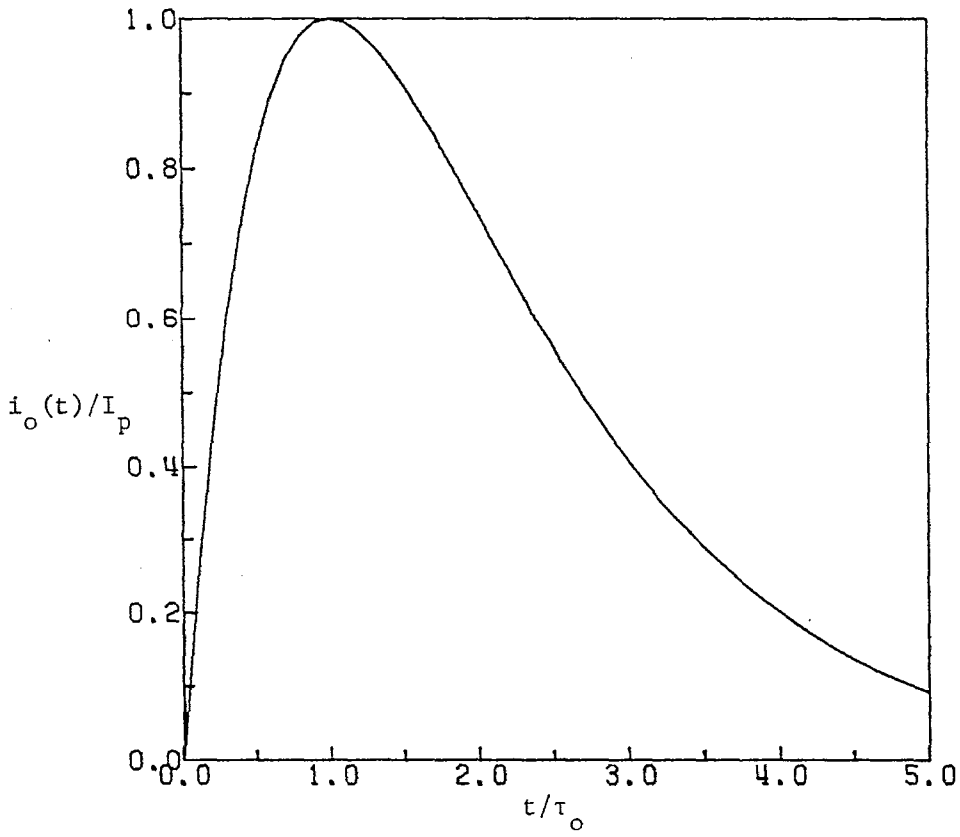

Figure 2. $i_o(t)/I_p$ vs. t/τ_o

$$2.\quad \left.\frac{\partial \tilde{\Psi}}{\partial \rho}\right|_{z=0+} - \left.\frac{\partial \tilde{\Psi}}{\partial \rho}\right|_{z=0-} = \frac{1}{s\varepsilon_o Z_s}\left.\frac{\partial^2 \tilde{\Psi}}{\partial \rho \partial z}\right|_{z=0} \tag{2.4b}$$

$$3.\quad \lim_{\rho \to 0} -2\pi\rho \frac{\partial \tilde{\Psi}}{\partial \rho} = \tilde{I}_o(s)\, U(z) \tag{2.4c}$$

The first condition implies that the radial electric field $\tilde{E}_\rho$ is continuous through the impedance sheet, and the second implies that the surface current density $\tilde{J}_{s\rho}$ is related to $\tilde{E}_\rho$ by

$$\tilde{E}_\rho(z=0) = Z_s \tilde{J}_{s\rho} \tag{2.5}$$

The third condition relates the field to the source current, whose Laplace transform $\tilde{I}_o(s)$ is

$$\tilde{I}_o(s) = \mathcal{L}[i_o(t)] = \frac{eI_p\tau_o}{(1 + s\tau_o)^2} \tag{2.6}$$

Curves of the magnitude and phase of $\tilde{I}_o(j\omega)/e\tau_o I_p$ as functions of $\omega\tau_o$ are given in Fig. 3.

Representations of $\tilde{\Psi}$ which are appropriate for each of the two regions of the problem and which satisfy the conditions of Eqs. (2.4a) and (2.4c) are

$$z>0:\quad \tilde{\Psi}(\rho,z,s) = \frac{\tilde{I}_o(s)}{2\pi} K_o\left(\frac{\rho s}{c}\right) + \int_o^\infty F(\lambda) J_o(\lambda\rho) e^{-z(s^2/c^2+\lambda^2)^{1/2}}\, d\lambda \tag{2.7a}$$

$$z<0:\quad \tilde{\Psi}(\rho,z,s) = -\int_o^\infty F(\lambda) J_o(\lambda\rho) e^{z(s^2/c^2+\lambda^2)^{1/2}}\, d\lambda \tag{2.7b}$$

in which $F(\lambda)$ is to be determined. $K_n(\cdot)$ denotes the modified Bessel function of the second kind and $J_n(\cdot)$ the Bessel function of order n, and the square roots appearing in Eqs. (2.7) are to be evaluated with

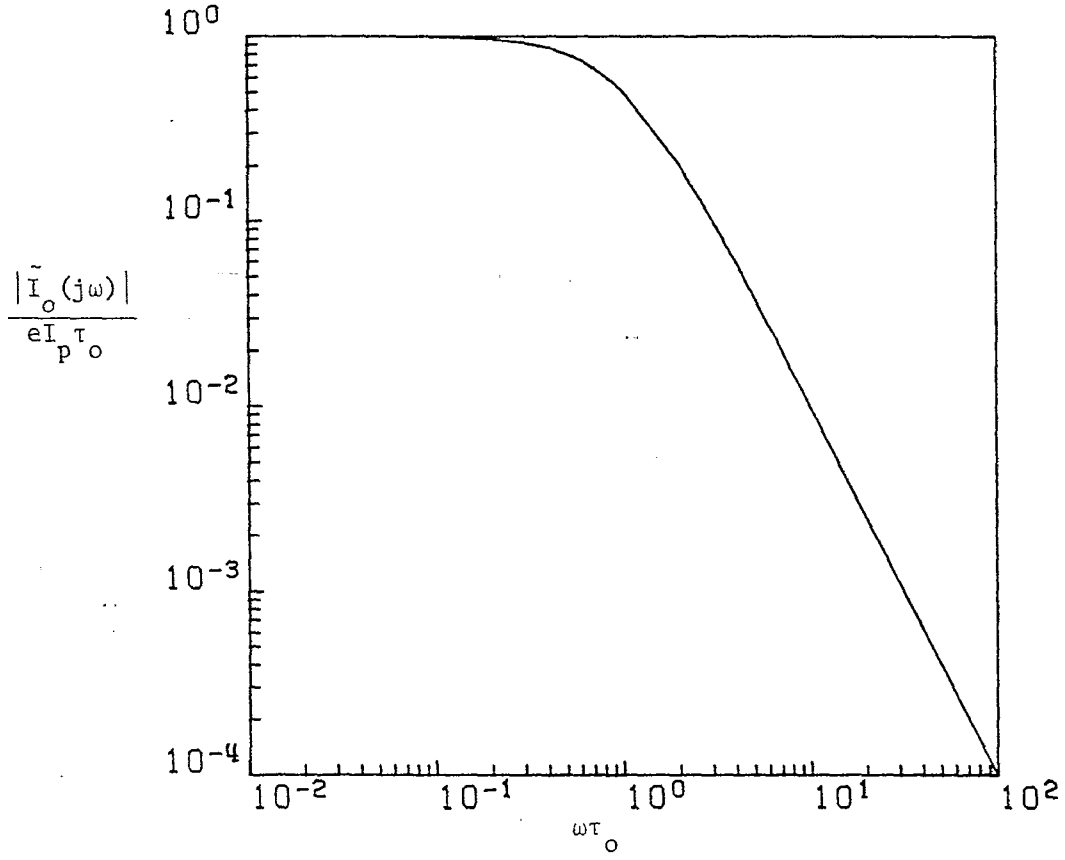

Figure 3a. Magnitude of $\tilde{I}_o(j\omega)/e\tau_o I_p$ vs. $\omega\tau_o$

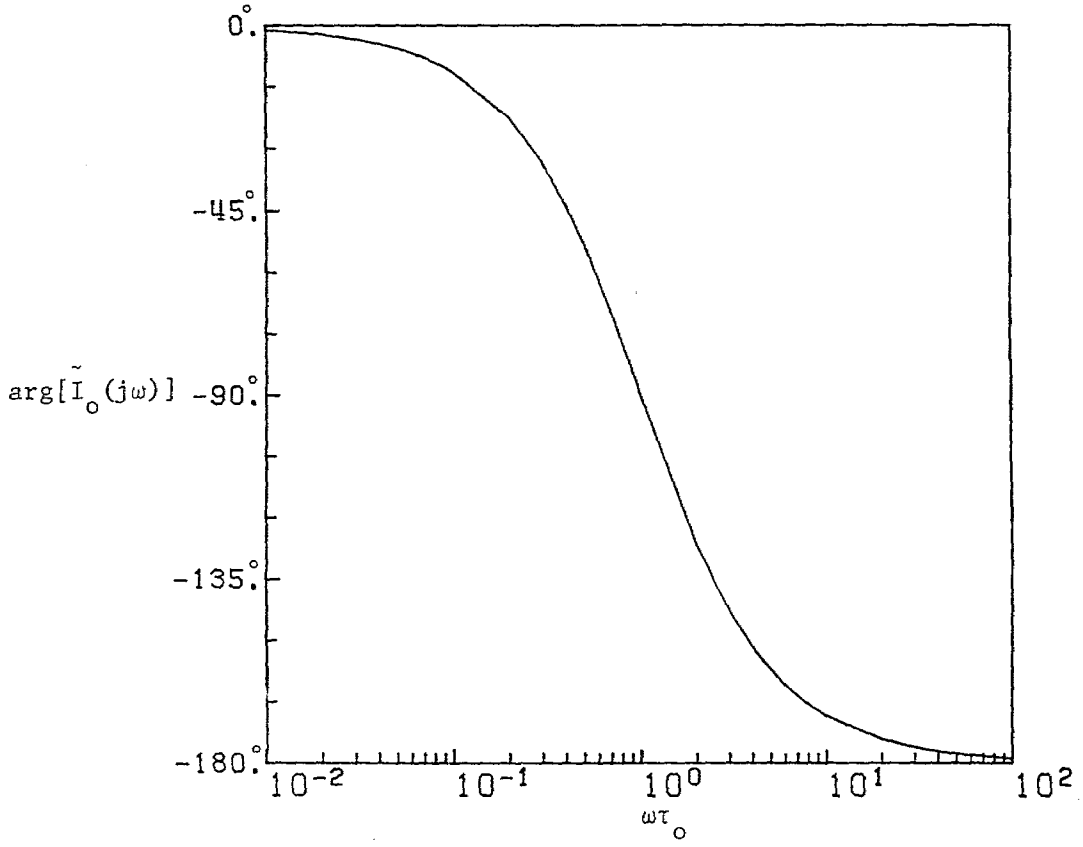

Figure 3b. Phase of $\tilde{I}_o(j\omega)$ vs. $\omega\tau_o$

$$\mathrm{Re}\left(\frac{s^2}{c^2} + \lambda^2\right)^{1/2} \geq 0 \tag{2.8}$$

Imposition of the condition given in Eq. (2.4b) on the representations for $\tilde{\Psi}$ in Eqs. (2.7) leads to the equation

$$\int_0^\infty F(\lambda)\ \left[\frac{c}{s}\sqrt{\frac{s^2}{c^2} + \lambda^2} + \frac{2Z_s}{Z_o}\right]\ \lambda J_1(\lambda\rho)d\lambda = \frac{-sI_o(s)}{2\pi c}\ \left(\frac{Z_s}{Z_o}\right)\ K_1\left(\frac{s\rho}{c}\right) \tag{2.9}$$

from which we readily obtain

$$F(\lambda) = \frac{-\lambda\tilde{I}_o(s)}{2\pi}\ \left(\frac{Z_s}{Z_o}\right)\ \left(\lambda^2 + \frac{s^2}{c^2}\right)^{-1}\ \left[\frac{c}{s}\sqrt{\frac{s^2}{c^2} + \lambda^2} + \frac{2Z_s}{Z_o}\right]^{-1} \tag{2.10}$$

when $\mathrm{Re}(s) > 0$, completing the formal solution of the problem. $Z_o = (\mu_o/\varepsilon_o)^{1/2}$ denotes the intrinsic impedance of free space.

The surface current density in the sheet has only a radial component, which is given by

$$\tilde{J}_{s\rho}(\rho,s) = \frac{-s\tilde{I}_o(s)}{2\pi c}\ K_1\left(\frac{s\rho}{c}\right) + \frac{s\tilde{I}_o(s)}{2\pi c}\ \int_0^\infty \frac{(2Z_s/Z_o)\lambda^2 J_1(\lambda\rho)d\lambda}{\left(\lambda^2 + \frac{s^2}{c^2}\right)\left[\left(\lambda^2 + \frac{s^2}{c^2}\right)^{1/2} + \frac{2s}{c}\ \frac{Z_s}{Z_c}\right]}$$

$$= \frac{-\tilde{I}_o(s)}{2\pi}\ \int_0^\infty \frac{\lambda^2 J_1(\lambda\rho)d\lambda}{\left(\lambda^2 + \frac{s^2}{c^2}\right)^{1/2}\left[\left(\lambda^2 + \frac{s^2}{c^2}\right)^{1/2} + \frac{2s}{c}\ \frac{Z_s}{Z_o}\right]} \tag{2.11}$$

The magnetic field $\tilde{H}_\phi$ in the region $z<0$ is

$$\tilde{H}_\phi(\rho,z,s) = \frac{-s\tilde{I}_o(s)}{2\pi c}\ \int_0^\infty \frac{(Z_s/Z_o)\lambda^2 J_1(\lambda\rho)e^{-|z|\sqrt{\lambda^2 + \frac{s^2}{c^2}}}\ d\lambda}{\left(\lambda^2 + \frac{s^2}{c^2}\right)\left[\left(\lambda^2 + \frac{s^2}{c^2}\right)^{1/2} + \frac{2s}{c}\ \frac{Z_s}{Z_o}\right]} \tag{2.12}$$

In the following sections, we evaluate the surface current density and the transmitted magnetic field in the time domain.

III. EVALUATION OF THE SURFACE CURRENT DENSITY

We begin with the second of the representations for $\tilde{J}_{s\rho}$ given in Eq. (2.11). First, we convert the integral from 0 to ∞ into an integral on $(-\infty,\infty)$, yielding

$$\tilde{J}_{s\rho}(\rho,s) = \frac{-\tilde{I}_o(s)}{4\pi} \int_{-\infty}^{\infty} \frac{\lambda^2 H_1^{(2)}(\lambda\rho)d\lambda}{(\lambda^2 + \frac{s^2}{c^2})^{1/2}[(\lambda^2 + \frac{s^2}{c^2})^{1/2} + \frac{2s}{c}\frac{Z_s}{Z_o}]} \qquad (3.1)$$

$H_n^{(2)}(\cdot)$ is the Hankel function of the second kind of order n. The integration contour runs slightly below the real axis over the interval $(-\infty,0)$, then along the real axis over $(0,\infty)$. We note that when $\mathrm{Re}(s) > 0$, the integrand is analytic in a strip $-\mathrm{Re}(s)/c < \mathrm{Im}(\lambda) < \mathrm{Re}(s)/c$, except along the branch cut on the negative real axis which arises from the Hankel function. Now when $\rho>0$ we may close the contour in the lower half plane with a semicircle whose radius is allowed to become infinitely large. This semicircle is interrupted by the branch cut originating at $\lambda = -js/c$, so that the total closed contour becomes the original contour ($-\infty \leq \lambda \leq \infty$), plus the semicircle at infinite radius in the lower half plane, plus the path around the branch cut. This closed contour is shown in Fig. 4. The branch cuts have been chosen to lie on the paths

$$\mathrm{Re}(\lambda^2 + \frac{s^2}{c^2})^{1/2} = 0 \qquad (3.2)$$

and the integrals are thus evaluated on paths lying entirely in the proper Riemann sheet of the cut λ-plane.

There are no singularities enclosed by the contour when Z_s is independent of λ. The pole at $(\lambda^2 + \frac{s^2}{c^2})^{1/2} + \frac{2s}{c}\frac{Z_s}{Z_o} = 0$ is located on

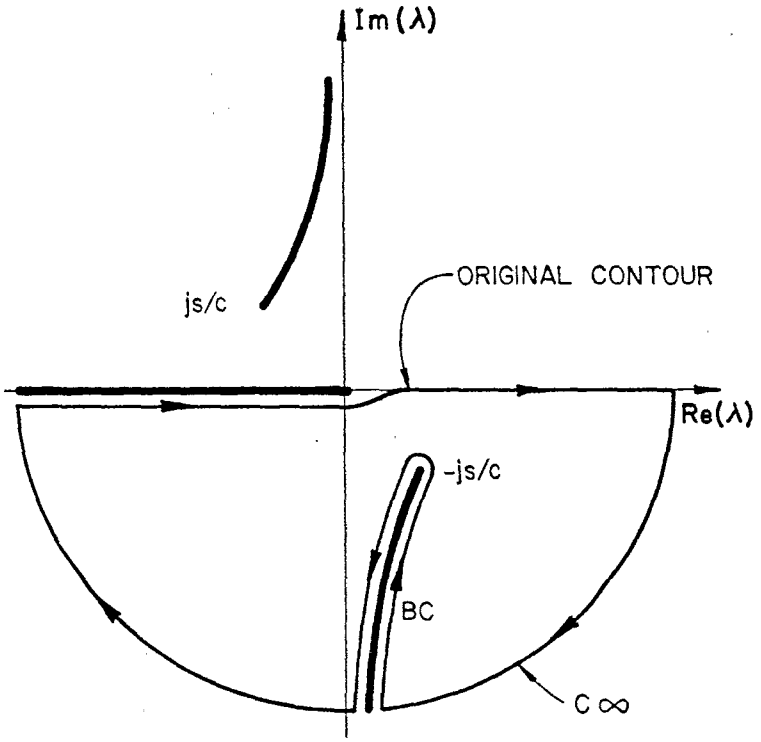

Figure 4. Integration contour in the complex λ-plane

the improper Riemann sheet of the cut λ-plane, so does not contribute to the integral. Thus since the integral over the semicircle of infinite radius vanishes, $\tilde{J}_{s\rho}(\rho,s)$ is given by

$$\tilde{J}_{s\rho}(\rho,s) = \frac{I_o(s)}{4\pi} \int_{BC} \frac{\lambda^2 H_1^{(2)}(\lambda\rho)d\lambda}{(\lambda^2 + \frac{s^2}{c^2})^{1/2}[(\lambda^2 + \frac{s^2}{c^2})^{1/2} + \frac{2s}{c}\frac{Z_s}{Z_o}]} \tag{3.3}$$

where BC denotes that portion of the path in Fig. 4 around the branch cut in the lower half plane.

Now let us introduce the change of variable

$$u = \frac{jc}{s}\lambda \tag{3.4}$$

into the integral in Eq. (3.3). We thus obtain for $\tilde{J}_{s\rho}(s,\rho)$

$$\tilde{J}_{s\rho}(s,\rho) = \frac{s\tilde{I}_o(s)}{2\pi^2 c} \int_C \frac{u^2 K_1(u\frac{s\rho}{c})du}{(u^2-1)^{1/2}[-j(u^2-1)^{1/2} + 2\frac{Z_s}{Z_o}]} \tag{3.5}$$

where the integration contour C is shown in Fig. 5. The branch cuts in the u-plane are the lines

$$\mathrm{Im}(u^2-1)^{1/2} = 0 \tag{3.6}$$

and the upper sheet of the cut u-plane is that on which $\mathrm{Im}(u^2-1)^{1/2} < 0$. The integration path C can be broken up into a segment just above the cut, a segment just below the cut, and a circular path around the branch point at u=1. When $Z_s \neq 0$, there is no contribution from the branch point itself, so we obtain after some elementary manipulations

$$\tilde{J}_{s\rho}(\rho,s) = \frac{-s\tilde{I}_o(s)}{2\pi c} \int_1^\infty \frac{u^2 K_1(ux)}{(u^2-1)^{1/2}} \left[\frac{4z_s/\pi}{4z_s^2 + u^2 - 1}\right] du \tag{3.7}$$

in which $z_s \equiv Z_s/Z_o$ and the positive square root is to be taken.

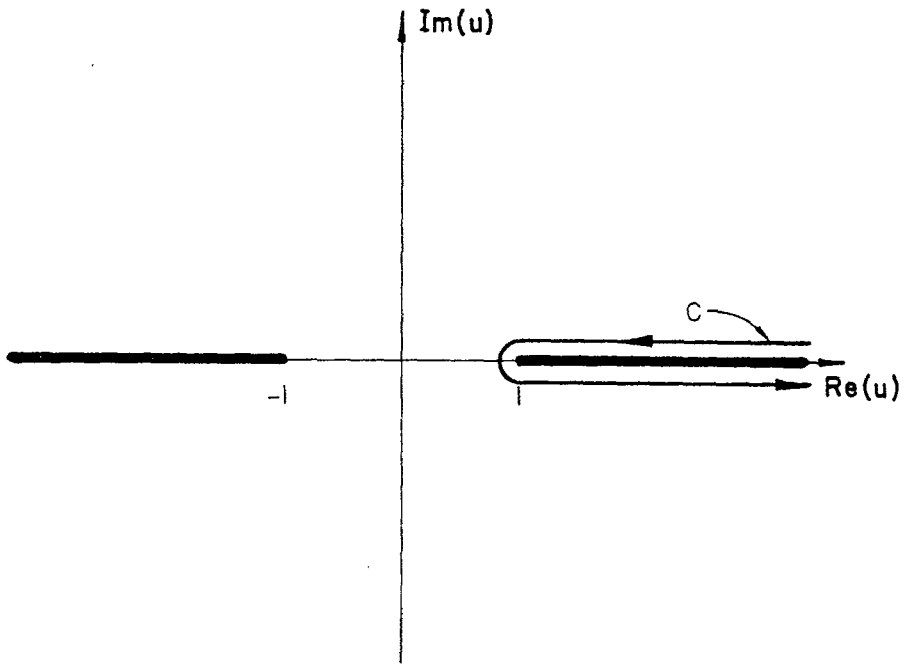

Figure 5. Integration contour in the complex u-plane

It is important to note that $\tilde{J}_{s\rho}$ does not vanish when $z_s \to 0$. The reason for this is that the function in square brackets in the integrand of Eq. (3.7) is actually a delta function in the limit $z_s \to 0$. This is clearly apparent if we introduce a final change of variable $v = (u^2-1)^{1/2}$, so that

$$\tilde{J}_{s\rho}(\rho,s) = \frac{-s\tilde{I}_o(s)}{2\pi c} \int_o^\infty (1+v^2)^{1/2} \, K_1\left(\frac{s\rho}{c}\sqrt{1+v^2}\right) \left[\frac{4z_s/\pi}{4z_s^2 + v^2}\right] dv \qquad (3.8)$$

Now consider the function $\Delta(z_s;v) = (4z_s/\pi)/(4z_s^2 + v^2)$. We have

$$\int_o^\infty \Delta(z_s;v)\, dv = 1 \qquad \text{(all } z_s\text{)} \qquad (3.9)$$

but when $z_s = 0$, $\Delta(z_s;v) = 0$ for all $v \neq 0$. Therefore $\Delta(z_s;v)$ in the limit $z_s \to 0$ is a "one-sided" delta function in the sense that

$$\int_o^\infty g(v) \lim_{z_s \to 0} \Delta(z_s;v)dv = g(0+) \qquad (3.10)$$

and so

$$\tilde{J}_{s\rho}(\rho;s)\Big|_{z_s=0} = \frac{-s\tilde{I}_o(s)}{2\pi c} K_1\left(\frac{\rho s}{c}\right) \qquad (3.11)$$

as we expect (cf. Eq. (2.11)).

The inverse Laplace transform of $K_1\left(\frac{\rho s}{c}\sqrt{1+v^2}\right)$ is [6]

$$L^{-1}\left[K_1\left(\frac{\rho s}{c}\sqrt{1+v^2}\,\right)\right] = \frac{ct}{\rho\sqrt{1+v^2}} \left\{\frac{U\left(t - \frac{\rho}{c}\sqrt{1+v^2}\right)}{\sqrt{t^2 - \frac{\rho^2}{c^2}(1+v^2)}}\right\} \qquad (3.12)$$

so that, since $i_o(t=0) = 0$,

$$J_{s\rho}(\rho,t) = -\frac{1}{2\pi\rho}\frac{di_o}{dt} * F_J(ct/\rho) \tag{3.13}$$

in which the "*" denotes convolution and

$$F_J(x) = x\,U(x-1)\int_o^{\sqrt{x^2-1}} \Delta(z_s;v)\,\frac{dv}{\sqrt{x^2-(1+v^2)}} \tag{3.14}$$

The integral in Eq. (3.14) can be evaluated to yield

$$F_J(x) = \frac{x\,U(x-1)}{\sqrt{x^2-(1-4z_s^2)}} \tag{3.15}$$

It will be noted that $(-1/2\pi\rho)F_J(ct/\rho)$ is the surface current density resulting from a unit step current $i_o(t)$, i.e.,

$$J_{s\rho}(\rho,t)\Big|_{i_o(t)=I_oU(t)} = \frac{-I_o}{2\pi\rho}F_J(ct/\rho) \tag{3.16}$$

Curves of $F_J(x)$ vs. x for various values of z_s are given in Fig. 6. When $i_o(t)$ is given by Eq. (2.1), $J_{s\rho}(\rho,t)$ can be expressed in integral form as

$$J_{s\rho}(\rho,t) = \frac{-I_p}{2\pi\rho}\int_o^{(t^2/\tau_o^2 - Q_o^2)^{1/2}} \left(1 - \frac{t}{\tau_o} + \sqrt{w^2+Q_o^2}\right)\exp\left(1 - \frac{t}{\tau_o} + \sqrt{w^2+Q_o^2}\right) \cdot \frac{w\,dw}{\sqrt{w^2+4z_s^2Q_o^2}} \tag{3.17}$$

when $t > \rho/c$; $J_{s\rho} = 0$ otherwise. Also, $Q_o \equiv \rho/c\tau_o$.

When the sheet impedance Z_s is of such a value as to be representative of graphite-epoxy composites or screened boron-epoxy composites, $2z_s$ is typically of order 10^{-4}. Furthermore, the maximum value of ρ which would

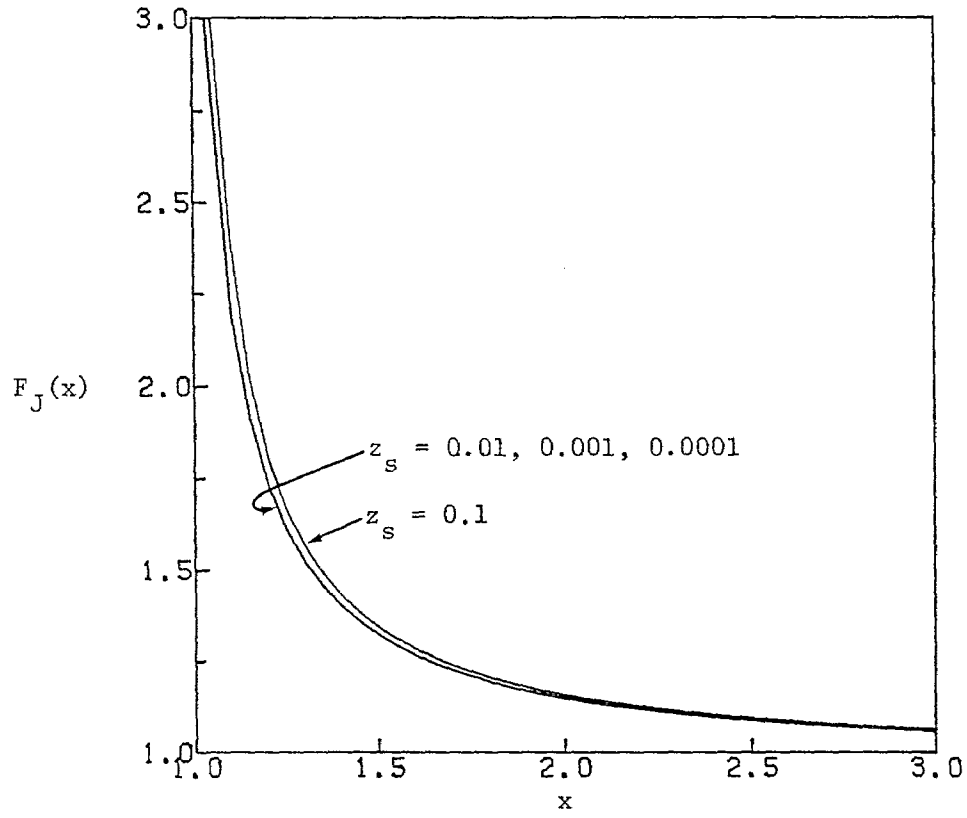

Figure 6. $F_J(x)$ vs. x; $z_s = 10^{-1}, 10^{-2}, 10^{-3}, 10^{-4}$

be of interest is of the order of 10 m. Thus when the transient current of Eq. (2.1) is applied, the quantity $\rho/c\tau_o$ is typically less than 10^{-1}. As a consequence, the surface current density in the sheet is very nearly identical to that which would exist if z_s were truly zero. This observation is borne out by numerical evaluation of the expression in Eq. (3.17). The resulting curves of $(-2\pi\rho)J_{s\rho}(\rho,t)$ are identical (within the accuracy of the plotter) to $i_o(t-\rho/c)$. Mathematically, this occurs because when $2z_sQ_o$ is very small, the function $w/\sqrt{w^2 + 4z_s^2Q_o^2}$ is essentially equal to unity over the range of the integration. Thus one is, in effect, performing a convolution of di_o/dt with a unit step; this yields a result proportional to $i_o(t-\rho/c)$.

IV. EVALUATION OF THE TRANSMITTED MAGNETIC FIELD

We begin with the transform representation for $\tilde{H}_\phi(\rho,z,s)$ in the region $z<0$ given in Eq. (2.12). Following a procedure similar to that used in the previous section, we transform the integral to

$$\tilde{H}_\phi(\rho,z,s) = \frac{js\tilde{I}_o(s)}{2\pi^2 c}\int_C \frac{z_s u^2 K_1(u\frac{s\rho}{c})e^{j\frac{s}{c}|z|\sqrt{u^2-1}}}{(u^2-1)[-j(u^2-1)^{1/2}+2z_s]}\,du \qquad (4.1)$$

where the contour C is shown in Fig. 5. Now we may convert the expression in Eq. (4.1) to a form in which the residue contribution at u=1 is displayed explicitly and the remainder is expressed as a definite integral:

$$\tilde{H}_\phi(\rho,z,s) = \frac{-s\tilde{I}_o(s)}{4\pi c}K_1(s\frac{\rho}{c})$$

$$+\frac{s\tilde{I}_o(s)}{\pi^2 c}z_s\int_1^\infty \frac{u^2K_1(u\frac{s\rho}{c})}{u^2-1}\left[\frac{\sqrt{u^2-1}\cos(\frac{s}{c}|z|\sqrt{u^2-1})+2z_s\sin(\frac{s}{c}|z|\sqrt{u^2-1})}{u^2-1+4z_s^2}\right]du$$

Finally, we introduce the change of variable $v=(u^2-1)^{1/2}$, yielding

$$\tilde{H}_\phi(\rho,z,s) = \frac{-s\tilde{I}_o(s)}{4\pi c}K_1(s\frac{\rho}{c})$$

$$+\frac{s\tilde{I}_o(s)}{4\pi c}\int_o^\infty \Delta(z_s;v)(1+v^2)^{1/2}K_1(\frac{s\rho}{c}\sqrt{1+v^2})[\cos(\frac{sv}{c}|z|)$$

$$+\frac{2z_s}{v}\sin(\frac{sv}{c}|z|)]dv \qquad (4.3)$$

One will again note the presence of the function $\Delta(z_s;v)$ in the integrand of Eq. (4.3). In the limit $z_s\to 0$, the integral and the residue contribution cancel, yielding a null result for $\tilde{H}_\phi$, as we would expect.

We now confine our attention to the determination of the magnetic field just below the sheet, $H_\phi(\rho,0-,t)$. This is done partly for mathematical simplicity, since the inverse Laplace transforms of $K_1(\alpha s)\cos\beta s$ and $K_1(\alpha s)\sin\beta s$ are rather complicated, and partly because our principal interest is in the near field. The minimum wavelength in the radiated field below the sheet will be around $c\tau_o$ (of order 10^2 m) and the physical distances $|z|$ of interest are of order 1 m.

Defining a function $F_H(x)$ by

$$F_H(x) = \frac{1}{2}\frac{x\,U(x-1)}{\sqrt{x^2-1}} - \frac{1}{2}\frac{x\,U(x-1)}{\sqrt{x^2-(1-4z_s^2)}} \tag{4.4}$$

we readily obtain

$$H_\phi(\rho,0-,t) = -\frac{1}{2\pi\rho}\frac{di_o}{dt} * F_H\left(\frac{ct}{\rho}\right) \tag{4.5}$$

Curves of $F_H(x)$ vs. x for various values of z_s are shown in Fig. 7. One will note that if $i_o(t) = I_p U(t)$, then $H_\phi(\rho,0-,t) = -I_p F_H(ct/\rho)/2\pi\rho$. When $i_o(t)$ is as given in Eq. (2.1), we find that $H_\phi(\rho,0-,t)$ is expressible as the integral

$$H_\phi(\rho,0-,t) = \frac{-I_p}{4\pi\rho}\int_o^{(t^2/\tau_o^2 - Q_o^2)^{1/2}} \left(1 - \frac{t}{\tau_o} + \sqrt{w^2+Q_o^2}\right)\exp\left(1 - \frac{t}{\tau_o} + \sqrt{w^2+Q_o^2}\right)\cdot$$

$$\left(1 - \frac{w}{\sqrt{w^2+4z_s^2Q_o^2}}\right)\,dw \tag{4.6}$$

when $t > \rho/c$ and $H_\phi = 0$ otherwise. $Q_o = \rho/c\tau_o$ as before.

Numerical computation of $-4\pi\rho H_\phi(\rho,0-,t)/I_p$ as a function of t/τ_o has been carried out for various values of $\rho/c\tau_o$ and z_s. For the range of parameters considered (i.e., small values of $\rho/c\tau_o$ and z_s) the resulting curves are indistinguishable from the function

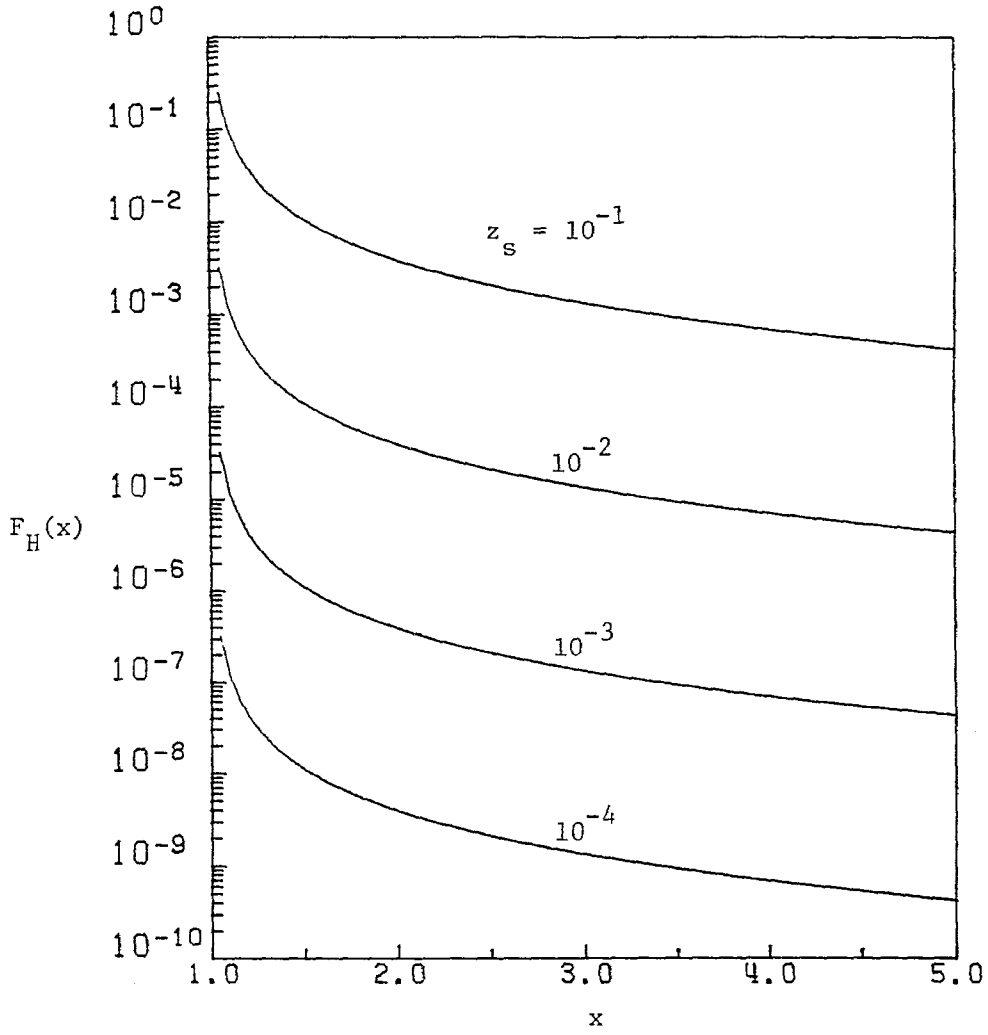

Figure 7. $F_H(x)$ vs. x; $z_s = 10^{-1}, 10^{-2}, 10^{-3}, 10^{-4}$

$$h(u) = 2z_s\left(\frac{\rho}{c\tau_o}\right)\frac{1}{I_p}\frac{di_o}{du} \tag{4.7}$$

where $u = t/\tau_o - \rho/c\tau_o$. The reason for this is easily seen. Consider the function

$$\hat{\Delta}(x;w) = \frac{1}{x}\left(1 - \frac{w}{\sqrt{w^2 + x^2}}\right) \tag{4.8}$$

This function has the property that

$$\int_o^\infty \hat{\Delta}(x;w)dw = 1 \qquad \text{(all x)}$$

and has a peak value of $1/x$ at $w=0$. The "width" of $\hat{\Delta}(x;w)$ is proportional to x. Thus in the limit as $x \to 0$, $\hat{\Delta}(x;w)$ approaches a Dirac delta-function. Hence when $2z_s \ll 1$,

$$H_\phi(\rho,0-,t) \approx \frac{-I_p}{4\pi\rho}(2z_s)\left(\frac{\rho}{c\tau_o}\right)\int_o^{(t^2/\tau_s^2 - \rho^2/c^2\tau_o^2)^{1/2}} \left(1 - \frac{t}{t_o} + \sqrt{w^2 + \rho^2/c^2\tau_o^2}\right).$$

$$\exp\left(1 - \frac{t}{\tau_o} + \sqrt{w^2 + \rho^2/c^2\tau_o^2}\right)\delta(w)\,dw \tag{4.9}$$

$$= \frac{-I_p}{4\pi\rho}(2z_s)\left(\frac{\rho}{c\tau_o}\right)\left(1 - \frac{t}{\tau_o} + \frac{\rho}{c\tau_o}\right)\exp\left(1 - \frac{t}{\tau_o} + \frac{\rho}{c\tau_o}\right)U\left(t - \frac{\rho}{c}\right)$$

from which Eq. (4.7) follows. A curve of $(\tau_o/I_p)di_o/dt$ is shown in Fig. 8.

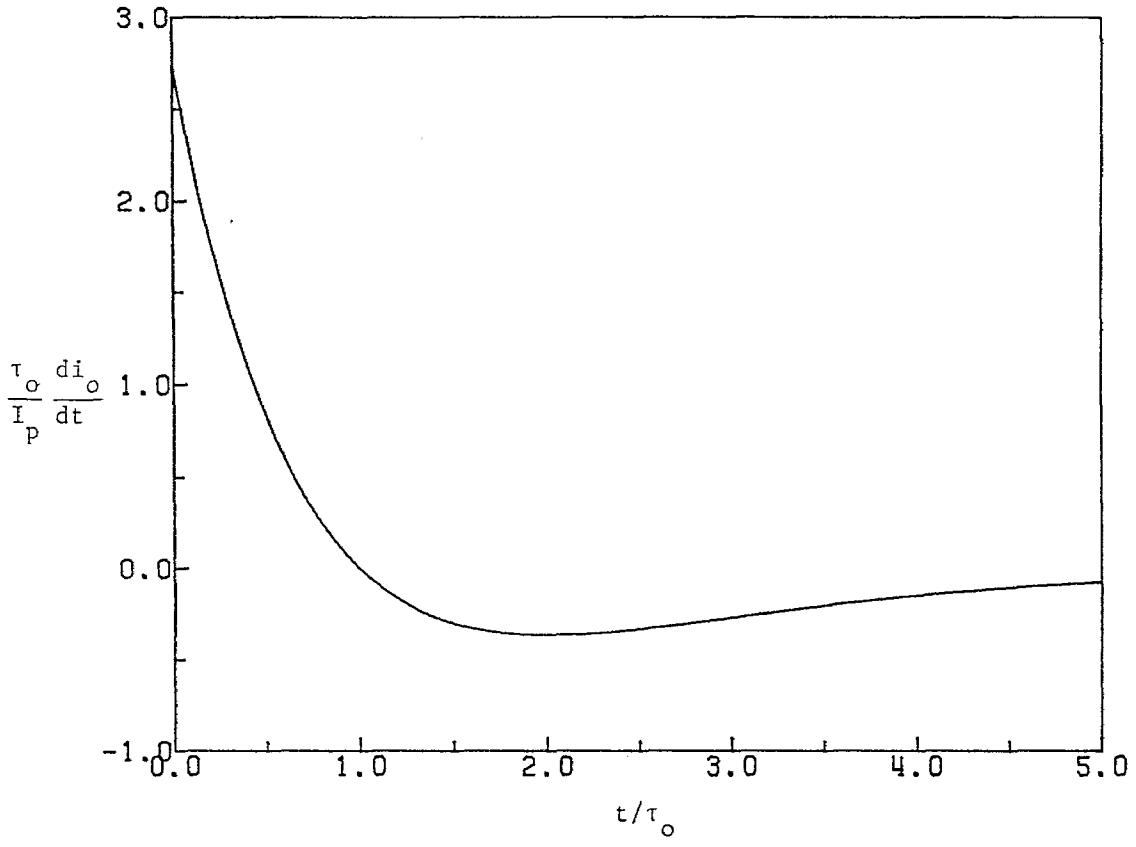

Figure 8. $(\tau_o/I_p)\,\frac{di_o}{dt}$ vs. t/τ_o

V. CONCLUDING REMARKS

We have found that when the normalized sheet impedance Z_s/Z_o is small in comparison to unity, the surface current density in the sheet induced by an applied injected filamentary current is given accurately by

$$J_{s\rho}(\rho,t) = -i_o(t-\rho/c)/2\pi\rho \tag{5.1}$$

where $i_o(t)$ denotes the time dependence of the injected current. Furthermore, the magnetic field just below the sheet is closely approximated by

$$H_\phi(\rho,0-,t) \simeq -(z_s/2\pi c)\frac{di_o}{dt'} \tag{5.2}$$

in which $t' = t - \rho/c$ and $z_s = Z_s/Z_o$. In both of these approximations, it is assumed that $\rho/c \ll \tau_o$, the characteristic rise time of the injected current.

We note that since the current density in the sheet is essentially identical to that which would exist if the sheet were perfectly conducting, the "ideal" current density may be used in calculations of, for example, the temperature rise as a function of position due to ohmic heating. It is simple to show that the temperature rise occurring because of an injected current of the form given in Eq. (2.1) is approximately given by

$$\Delta T = \frac{\alpha^2}{K}\frac{Z_s e^2 I_p^2 \tau_o}{16\pi^2\rho^2 d} \tag{5.3}$$

in which α^2 is the thermal diffusivity of the conducting material and K is its thermal conductivity. Thus immediately after the passage of the wave of surface current density, the temperature of the panel will be approximately $T_o + \Delta T(\rho)$, in which T_o is the panel temperature before the current was injected.

References

[1] L. Allen, W. F. Walker, and K. R. Siarkiewicz, "An Investigation of the Electromagnetic Properties of Advanced Composite Materials," IEEE 1976 International Symposium on Electromagnetic Compatibility Record, pp. 174-179.

[2] K. F. Casey, "Advanced Composite Materials and Electromagnetic Shielding," IEEE 1978 International Symposium on Electromagnetic Compatibility Record, pp. 228-232.

[3] K. F. Casey, "EMP Penetration through Advanced Composite Skin Panels," Interaction Notes, Note 315, December 1976.

[4] K. F. Casey, "Equivalent Sheet Impedance of a Bonded-Mesh Screen on an Anisotropic Half-Space," presented at 1977 USNC/URSI Meeting, Stanford, CA, June 1977.

[5] L. Allen, W. J. Gajda, et al., "A Technology Plan for Advanced Composites," RADC-TR-76-206, July 1976.

[6] Bateman Manuscript Project, Tables of Integral Transforms, Vol. I, McGraw-Hill, New York, 1954, p. 277.